⌘ *Author's Choice*

THE JOURNAL OF BIOLOGICAL CHEMISTRY VOL. 286, NO. 38, pp. 33053–33060, September 23, 2011

NrdH-Redoxin Protein Mediates High Enzyme Activity in Manganese-reconstituted Ribonucleotide Reductase from *Bacillus anthracis*[*] [S]

Received for publication, June 30, 2011, and in revised form, August 2, 2011 Published, JBC Papers in Press, August 6, 2011, DOI 10.1074/jbc.M111.278119

Mikael Crona[‡], Eduard Torrents[‡§1], Åsmund K. Røhr[¶1], Anders Hofer[‖], Ernst Furrer[‡2], Ane B. Tomter[¶], K. Kristoffer Andersson[¶], Margareta Sahlin[‡], and Britt-Marie Sjöberg[‡3]

From the [‡]Department of Molecular Biology and Functional Genomics, Arrhenius Laboratories for Natural Sciences, Stockholm University SE-10691 Stockholm, Sweden, [§]Cellular Biotechnology, Institute for Bioengineering of Catalonia, Baldiri Reixac 15-21, ES-08080 Barcelona, Spain, the [¶]Department of Molecular Biosciences, University of Oslo, NO-0316 Oslo, Norway, and the [‖]Department of Medical Biochemistry and Biophysics, Umeå University, SE-90187 Umeå, Sweden

Background: Class Ib ribonucleotide reductase of the severe pathogen *Bacillus anthracis* can be loaded with manganese or iron.
Results: The manganese form was 10-fold more active than the iron form in the presence of the physiological protein NrdH-redoxin.
Conclusion: The manganese form is important in the life cycle of *B. anthracis.*
Significance: The physiologically relevant form of ribonucleotide reductase controls *B. anthracis* proliferation and survival.

Bacillus anthracis **is a severe mammalian pathogen encoding a class Ib ribonucleotide reductase (RNR). RNR is a universal enzyme that provides the four essential deoxyribonucleotides needed for DNA replication and repair. Almost all *Bacillus* spp. encode both class Ib and class III RNR operons, but the *B. anthracis* class III operon was reported to encode a pseudogene, and conceivably class Ib RNR is necessary for spore germination and proliferation of *B. anthracis* upon infection. The class Ib RNR operon in *B. anthracis* encodes genes for the catalytic NrdE protein, the tyrosyl radical metalloprotein NrdF, and the flavodoxin protein NrdI. The tyrosyl radical in NrdF is stabilized by an adjacent Mn_2^{III} site (Mn-NrdF) formed by the action of the NrdI protein or by a Fe_2^{III} site (Fe-NrdF) formed spontaneously from Fe^{2+} and O_2. In this study, we show that the properties of *B. anthracis* Mn-NrdF and Fe-NrdF are in general similar for interaction with NrdE and NrdI. Intriguingly, the enzyme activity of Mn-NrdF was approximately an order of magnitude higher than that of Fe-NrdF in the presence of the class Ib-specific physiological reductant NrdH, strongly suggesting that the Mn-NrdF form is important in the life cycle of *B. anthracis*. Whether the Fe-NrdF form only exists *in vitro* or whether the NrdF protein in *B. anthracis* is a true cambialistic enzyme that can work with either manganese or iron remains to be established.**

The essential enzyme ribonucleotide reductase (RNR)[4] catalyzes a key reaction in the synthesis of the necessary deoxyribonucleotide (dNTP) building blocks for DNA synthesis and is essential in all cells and organisms, except a few parasites or obligate intracellular endosymbionts (1–3). Three major classes denoted I, II, and III are known within the RNR enzyme family and differ primarily in cofactor requirement, quaternary structure, free radical chemistry, and oxygen dependence. All RNRs employ a radical chemistry reaction mechanism, and almost all are regulated via sophisticated allosteric mechanisms keeping a balanced supply of all dNTPs. Despite extensive amino acid sequence differences, the three-dimensional core structure is preserved and points to a common evolutionary history for all three RNR classes (4–6). *Bacillus anthracis*, the causative agent of anthrax disease, encodes an oxygen-dependent class I RNR and an oxygen-sensitive class III RNR in its genome. However, the gene for the class III-specific activase was reported to be a pseudogene (7). We have earlier shown that specific inhibition of the *B. anthracis* class I RNR via the radical scavenger compound *N*-methylhydroxylamine efficiently knocks out growth of the organism (8).

The vast majority of class I RNRs consist of a large α-component that harbors the active site and two types of binding sites for allosteric nucleoside triphosphate effectors and a small β-component that harbors a stable tyrosyl radical close to a diiron-oxo site. Common to all studied class I RNRs is that they

[*] This work was supported by grants from the Swedish Cancer Foundation and the Swedish Research Council (to B.-M. S.), from the Fondo de Investigación Sanitaria from the Spanish Ministerio de Ciencia e Innovación (Grant PI081062), the ERA-NET PathoGenoMics, and the Ramón y Cajal program (to E. T.), from the EMBIO/MLS at the University of Oslo to (to Å. K. R.), from the Carl Trygger Foundation (to A. H.), and from the Research Council of Norway (Grants 177661/V30) and Norwegian Cancer Society (to K. K. A.).
⌘ *Author's Choice*—Final version full access.
[S] The on-line version of this article (available at http://www.jbc.org) contains supplemental Figs. S1–S9.
[1] Both authors contributed equally to this work.
[2] Present address: Federal Office for the Environment (FOEN), Waste Management, Chemicals and Biotechnology Division, CH-3003 Berne, Switzerland.
[3] To whom correspondence should be addressed: Dept. of Molecular Biology and Functional Genomics, Stockholm University, Svante Arrhenius väg 20C, SE-106 91 Stockholm, Sweden. E-mail: britt-marie.sjoberg@molbio.su.se.

[4] The abbreviations used are: RNR; ribonucleotide reductase; Fe-NrdF, iron-containing NrdF; Mn-NrdF, manganese-containing NrdF; GEMMA, gas-phase electrophoretic mobility macromolecular analysis; EU, enzyme unit(s).

are able to form an $\alpha_2\beta_2$ holoenzyme complex, which in prokaryotes seems to be the main active form. Species-dependent larger complexes can also be induced such as the allosterically inhibited $\alpha_4\beta_4$ form in *Escherichia coli* (9). Class I RNRs also encompass a few subclasses; the class Ib RNRs are restricted to a few phyla among eubacteria and to some bacteriophages, whereas the canonical class I RNRs (sometimes called class Ia) are found in almost all eukaryotes, in several eubacterial phyla, in a few archaea, and in some dsDNA viruses (2). Class Ib RNRs are distinguished by a special operon structure that in addition to the α- and β-polypeptides encoded by the *nrdE* and *nrdF* genes also encodes a flavodoxin protein in the *nrdI* gene, and in most operons, the *nrdH* gene encoding a low molecular mass redoxin protein that is specific for reduction of the class Ib RNR. The NrdE protein differs from the canonical class I α-component by having only one type of binding site for allosteric effectors, and the NrdF protein was recently shown to differ from the canonical β-component in its capacity to stabilize the tyrosyl radical by either forming a dimanganese-oxo center or a diiron-oxo center (1, 10, 11). Recent studies have also identified a role for the hitherto enigmatic flavodoxin protein NrdI (12–14), which is required for the manganese-dependent activation of NrdF *in vitro* (15, 16), but not for the iron-dependent *in vitro* activation of NrdF. Proficient genetic studies in *E. coli* showed that the Ib RNR is used under oxidative stress or iron limitation, when the canonical class Ia RNR is nonfunctional (17).

The class Ib RNR operon structure in the *Bacillus cereus* group (*B. anthracis, B. cereus, Bacillus mycoides, Bacillus thuringiensis,* and *Bacillus weihenstephanensis* spp.) encodes the *nrdI*, *nrdE*, and *nrdF* genes (*cf.* supplemental Fig. S1 for the *B. anthracis* operon), but the class Ib-specific *nrdH* gene is encoded elsewhere on the chromosome (7). Likewise, the gene for thioredoxin reductase that transfers electrons from NADPH to NrdH-redoxin is located elsewhere on the chromosome (7). In this study, we show that the manganese-dependent class Ib RNR in *B. anthracis* has up to 10-fold higher enzyme activity as compared with the iron-dependent form of the enzyme in presence of the physiological reductant NrdH. Apart from this critical and conceivably physiologically important difference, the Mn-NrdF and Fe-NrdF forms of *B. anthracis* class Ib RNR have similar characteristics *in vitro*. Our results conceivably point to the essential role of the manganese-dependent form of class Ib RNR in *B. anthracis* and the *B. cereus* group, and it remains to be shown whether the iron-dependent form also has a role *in vivo*.

EXPERIMENTAL PROCEDURES

Materials—DNA manipulations were carried out using standard protocols (18). *E. coli* strains DH5α (Stratagene) and Rosetta (DE3) (Novagen) were used for cloning and protein expression experiments, respectively. Wild type *B. anthracis* Sterne 7700 pXO1$^-$/pXO2$^-$ (lacking both virulence plasmids) was obtained from the Swedish Defense Research Agency. *E. coli* strains were routinely grown in LB medium at 37 °C, and *B. anthracis* was grown in brain heart infusion medium (BD Biosciences) at 37 °C. When required, antibiotics and chromogenic substrates were added at the following concentrations: 50 μg/ml ampicillin, 20 μg/ml chloramphenicol, 50 μg/ml kanamycin, and 30 μg/ml 5-bromo-4-chloro-3-indolyl-β-D-galactopyranoside (X-Gal).

Construction of a B. anthracis NrdE Expression Vector—To amplify the NrdE protein, the homing endonuclease gene present in the group I intron in the *B. anthracis nrdE* gene (19) had to be removed due to its toxicity in cloned *nrdE* constructs. In two consecutive PCR reactions using *B. anthracis* genomic DNA (8) as template, the first pair of primers 1 (5′-ACCATGGTGCGACACATTGAACTG-3′) and 2 (5′-AAAAAACTCGAGATTCCACTTCACCCAAG-3′) was used to amplify a 985-bp fragment comprising exon 1 and the 5′ part of the intron. A second pair of primers 3 (5′-AAAAAACTCGAGTACTATCCAATAACT-3′) and 4 (5′-AGGATCCTATTAAACAGTACAAGCC-3′) was used to amplify a 1502-bp fragment comprising the 3′ part of the intron and exon 2 (supplemental Fig. S1). Both fragments were gel-purified, digested with XhoI, ligated using T4 DNA ligase (Fermentas), and used as templates for a second PCR reaction using only primers 1 and 4. The entire *nrdE* sequence without the endonuclease-coding region was cloned into pGEM-T-easy (Promega) and sequenced to ensure that no mutations were introduced by the PCR reactions. After digestion with NcoI and BamHI, the *nrdE* gene was cloned in the pET28a vector (Novagen) and named pETS146.

Expression and Purification of Recombinant B. anthracis NrdE, ApoNrdF, and NrdI Proteins—NrdE protein was produced in *E. coli* Rosetta (DE3) using the pET system (pETS146) according to standard procedures (Novagen). The growth temperature was 30 °C, and induction was performed for 4 h with 0.7 mM isopropyl-β-D-thiogalactopyranoside. The protein crude extract was prepared as described earlier for the NrdF protein (8). The most abundant band was the NrdE protein (predicted molecular mass 79.8 kDa), demonstrating that the *B. anthracis* intron is efficiently spliced during overproduction in *E. coli* (supplemental Fig. S2). NrdE was enriched by chromatography on a HiLoad® 16/10 Phenyl Sepharose® column (GE Healthcare) by applying a 0.75–0 M gradient of ammonium sulfate in buffer containing 50 mM Tris-HCl, pH 7.5, and 2 mM DTT (buffer A). Fractions were analyzed by SDS gel electrophoresis, and those with the *B. anthracis* NrdE band were concentrated and extensively washed with buffer A using a Centricon-50 tube (Millipore). All steps were carried out on ice or at 4 °C. From a typical experiment, we obtained 13–16 mg of pure NrdE protein from 5 liters of bacterial cell culture with a purity of ≥95% (supplemental Fig. S2). *B. anthracis* NrdF protein was purified using Rosetta (DE3) cells containing pETS145 and was obtained as apoprotein (lacking a metal center) as described previously (8). *B. anthracis* NrdI protein was purified using Rosetta (DE3) cells containing pETS153 as described previously (14).

Expression and Purification of Recombinant B. cereus NrdH, Thioredoxin Reductase, NrdE, NrdF, and NrdI—B. cereus ATCC 14579 NrdH-redoxin (BC3987), thioredoxin reductase (BC5159), NrdE (BC1354), NrdF (BC1355), and NrdI (BC1353) were expressed and purified as described previously (13, 20–22). In brief, genes were cloned into the pET22b vector and transformed into BL21 (DE3) cells. Transformed BL21 (DE3)

cells containing pET22b-NrdI, -NrdH, -NrdE, or -NrdF were grown in TB medium containing 100 μg/ml ampicillin. Protein expression was induced by adding 0.8–1 mM isopropyl-1-thio-β-D-galactopyranoside, and cells were harvested by centrifugation after 12–16 h at 20 °C. The frozen cell paste was disintegrated using an X-press® (23), extracted with a solution containing 50 mM Tris-HCl, pH 7.5, and 10 mM EDTA (buffer B), and cleared from nucleic acids by streptomycin sulfate (2.5%) precipitation. Proteins were concentrated by ammonium sulfate precipitation using 0.29 mg/ml for NrdF and 0.43 mg/ml for NrdE, NrdH, and NrdI before desalting and purification by strong anion exchange chromatography (HiTrap Q HP) with a 0–0.5 M KCl gradient in buffer B. When required, a final purification step with Superdex-200 equilibrated in buffer B was used. For NrdE, all steps also included 2 mM DTT. *B. cereus* NrdH (78 residues) is 98% identical to the corresponding *B. anthracis* protein (BAS3897, annotated "glutaredoxin family protein") and differs at two positions: A28V and D59N, none of which is close to the active site of NrdH.

Metal Reconstitution of ApoNrdF with Manganese or Iron—ApoNrdF was incubated with four Mn^{2+}/dimer at room temperature for at least 5 min under anaerobic conditions, after which reduced NrdI was added and oxygen was admitted after 5–10 min. The ratio of NrdF:NrdI was ~1:1 to enable monitoring of the tyrosyl radical formed after reaction with oxygen in the resulting light absorption spectrum. Reduction of $NrdI_{ox}$ was performed by the addition of dithionite. Reduction of a mixture of Mn^{II}_2-NrdF and $NrdI_{ox}$ with dithionite worked equally well and was used in some experiments. Oxygen was either added by bubbling pure oxygen through the sample with a Hamilton syringe or simply by opening the reaction vessel to air. *In vitro* incorporation of iron to the NrdF protein was performed as described earlier (8).

Separation of Mn-NrdF/Tyr• and $NrdI_{ox}$ after Reconstitution—Mn-NrdF was separated from NrdI using a MonoQ column (GE Healthcare) and a 0–1 M KCl gradient in buffer A. NrdI eluted in the beginning of the gradient and Mn-NrdF eluted in two peaks, one lacking the radical and one containing 0.5 Tyr• per Mn-NrdF dimer (supplemental Fig. S3).

UV-visible Spectroscopy of Metal Reconstituted NrdF—UV-visible spectra were recorded on a PerkinElmer Life Sciences Lambda 35 spectrophotometer typically in 100-μl volume and with 10 μM NrdF dimer. If necessary, the spectra were baseline-corrected to zero absorbance at 750 nm, and for the isolated tyrosyl radical spectrum (see Fig. 1, *trace C*, *upper graph*), glitches in the spectrum were removed manually for better appearance.

The tyrosyl radicals in the different preparations were determined from the dropline procedure using $\epsilon = 2.11\ mM^{-1}cm^{-1}$ (12). In mixtures with NrdI, the spectrum of $NrdI_{ox}$ was subtracted from the composite spectrum before radical determination.

RNR Enzymatic Activity—Initial enzyme assays with *B. anthracis* NrdE and NrdF using conditions described for other class Ib proteins (24–27) gave very low specific activity, indicating that assay conditions were suboptimal. Interestingly, the DTT requirement had a surprisingly sharp optimum at ~8 mM and distinct inhibition at higher DTT concentrations (supplemental Fig. S4*A*). The pH profile was notably narrow, with optimal activity at pH 7.5 (supplemental Fig. S4*B*). Attempts to further increase the enzyme activity (additions of *B. anthracis* crude extract and microaerobic and anaerobic assays) failed (data not shown). With optimized assay conditions, *B. anthracis* RNR activity was determined in 50-μl reactions containing 0.5–1 μM Mn-NrdF (reconstituted with 1:1 NrdI), 4 μM NrdE, 50 mM Tris-HCl, pH 7.5, 20 mM magnesium acetate, 0.2 mM dATP and 0.8 mM [^{3}H]CDP (37,956 cpm/(min × nmol)). Reducing systems were 10 mM DTT, 5 μM *B. cereus* NrdH + 10 mM DTT, or 5 μM *B. cereus* NrdH + 0.5 μM thioredoxin reductase + 0.4 mM NADPH. Following 10 min of incubation at 37 °C, the reaction was terminated by adding 0.5 ml of 1 M perchloric acid, and the formed dCDP was analyzed as described (28). One enzyme unit (EU) is equivalent to 1 nmol of dCDP produced per min. Specific activity is expressed as EU per mg of NrdF protein.

GEMMA Analysis—All proteins were equilibrated on G-25 columns (GE Healthcare) into a buffer containing 20 mM ammonium acetate, pH 7.8 (plus 2 mM DTT and 0.005% (v/v) Tween 20 for NrdE protein solutions). Protein concentrations were 0.02–0.04 mg/ml (NrdE), 0.005–0.02 mg/ml (NrdF), 0.006–0.012 mg/ml (NrdI), and 0.004–0.008 mg/ml (NrdH). Substrate and/or effector nucleotides (1:1 nucleotide/magnesium acetate ratio) were included at 25–50 μM. The GEMMA system contained the following components: a 3480 electrospray aerosol generator, a 3080 electrostatic classifier, a 3085 differential mobility analyzer, and a 3025A ultrafine condensation particle counter (TSI Corp., Shoreview, MN). The parameters used in the GEMMA system were similar to those described previously (29). A capillary pressure drop of 1.4–2.0 p.s.i. was used to minimize a broad nucleotide peak in the beginning of the graphs and nonspecific binding of nucleotides to the generated protein particles (the nucleotide-induced molecular mass determination error was thereby minimized to a few percentages). When several experiments were plotted in the same graph, the baseline of each experiment was plotted 300–800 units apart for clarity.

Gel Filtration—To estimate the molecular mass of the NrdE and NrdF proteins alone or in combination at high protein concentrations (1.5–5 mg/ml NrdE and 0.75–5 mg/ml NrdF) and with high nucleotide concentration (0.2 mM dATP), we used a 2-ml column of Superdex-200 (GE Healthcare) chromatographed at 0.1 ml/min in buffer containing 50 mM Tris-HCl, pH 7.5, 8 mM DTT, 20 mM magnesium acetate, and 100 mM NaCl. Molecular mass markers (bovine serum albumin, 66 kDa; alcohol dehydrogenase, 150 kDa; β-amylase, 200 kDa; apoferritin, 443 kDa; thyroglobulin, 669 kDa, all purchased from Sigma) were run on the same column to obtain a standard curve for determination of molecular masses.

Surface Plasmon Resonance Analysis of the NrdF/NrdI Interaction—The detailed procedure has been published (30) but is briefly described here. The surface plasmon resonance (SPR) protein/protein interaction studies were performed using a Biacore 3000 biosensor instrument (GE Healthcare). A sterile-filtered and degassed mixture of 50 mM HEPES, pH 7.4, 0.15 M NaCl, 1 mM EDTA, 10 mM $MgCl_2$, 2 mM DTT, and 0.005% (v/v) surfactant P20 was used as running buffer.

B. anthracis NrdF was biotinylated with EZ-Link Sulfo-NHS-LC-LC-Biotin from Pierce Biotechnology Inc. and retained 88% of its enzymatic activity. The biotinylated NrdF protein (ligand) was subsequently immobilized to streptavidin-coated sensor chips (GE Healthcare). A biotin-deactivated flow cell was used as a reference cell in the experiments. NrdI protein solutions of different concentrations (analyte) were injected at a flow rate of 30 μl/min over the immobilized NrdF protein, and the binding was monitored. Bound NrdI protein was removed from the immobilized NrdF protein by injection of 15 μl of 0.5 M KCl followed by dissociation in running buffer. Data were analyzed using steady-state affinity calculations within the BIAevaluation 3.2 software (GE Healthcare).

RESULTS

Reconstitution of B. anthracis ApoNrdF with Manganese Requires Flavodoxin Protein NrdI—ApoNrdF (NrdF without bound metal ions) was reconstituted with either Mn^{2+} or Fe^{2+}. Initially, we attempted to oxidize bound Mn^{II} with O_2 or peroxide, but such experiments were not successful until the RNR-specific flavodoxin protein NrdI was included. After reduction of a Mn^{II}_2-NrdF/NrdI mixture with a slight excess of dithionite followed by O_2 oxidation, a distinct band appeared at 408 nm in the visible spectrum, indicating that a tyrosyl radical had formed concomitant with oxidation of the reduced $NrdI_{hq}$ to $NrdI_{ox}$ with an oxidized flavin absorption (Fig. 1, *trace A*, *upper graph*). The activated Mn-NrdF/Tyr$^{\bullet}$ protein (Fig. 1, *trace C*, *upper graph*) could be separated from $NrdI_{ox}$ (Fig. 1, *trace B*, *upper graph*) on a Mono-Q anion exchange column, and a radical content of 0.50 per Mn-NrdF dimer was calculated. Incubation of the apoNrdF protein with ferrous ions in the presence of O_2 gave a reconstituted Fe-NrdF/Tyr$^{\bullet}$ protein (Fig. 1, *trace B*, *lower graph*) with a radical content of 0.59 per Fe-NrdF dimer. The tyrosyl radical spectrum shown (Fig. 1, *trace C*, *lower graph*) was achieved by subtraction of a hydroxylamine-treated sample from the spectrum in *trace B* (Fig. 1, *lower graph*). Inclusion of reduced $NrdI_{hq}$ during iron reconstitution of apoNrdF had no effect on the radical yield (Fig. 1, *trace A*, *lower graph*).

Weak Interactions between NrdF and NrdI—We used SPR with immobilized NrdF proteins to determine the affinity of NrdI for Mn-NrdF as compared with Fe-NrdF and apoNrdF. All NrdF/NrdI interactions were weak, but Mn-NrdF formed a slightly tighter interaction with NrdI as compared with the other NrdF forms (Table 1 and supplemental Fig. S5). The weak NrdF/NrdI interactions were also verified by GEMMA. NrdI was predominantly a monomer (Fig. 2, *trace A*), whereas both Mn-NrdF/Tyr$^{\bullet}$ and Fe-NrdF/Tyr$^{\bullet}$ were predominantly dimers (Fig. 2, *traces B* and *D*). The experimental (GEMMA and gel filtration) and theoretical molecular masses for the different forms are shown in Table 2. When NrdI was mixed with either Mn-NrdF or Fe-NrdF, a minor peak plausibly corresponding to a complex of a NrdF dimer and a NrdI monomer was formed (Fig. 2, *traces C* and *E*). However, most of the protein components in these mixtures were not engaged in an NrdF/NrdI complex, as expected from the weak interaction between NrdF and NrdI measured by SPR.

Mn-NrdF and Fe-NrdF Form $\alpha_2\beta_2$ Complexes with NrdE—The interaction between NrdE and either of the NrdF forms was studied primarily by SPR and GEMMA. No significant difference was found in the interaction strength between the NrdE protein and the different NrdF forms in SPR (Table 3 and supplemental Fig. S6). The GEMMA analyses showed that NrdE is predominantly a monomer in the absence of effector nucleotide but that the dimer-to-monomer ratio increases in the presence of the positive allosteric effector dATP (Fig. 3). Dimerization of NrdE was also promoted by the allosteric effectors dGTP and dTTP, but not by 50 μM substrate (supplemental Fig. S7). When NrdE was mixed with NrdF, a fraction of the protein components formed a complex corresponding to an $\alpha_2\beta_2$ composition (Fig. 3, *traces C–F*). Importantly, as indicated by the SPR data, both Mn-NrdF and Fe-NrdF behaved very similar in these mixtures.

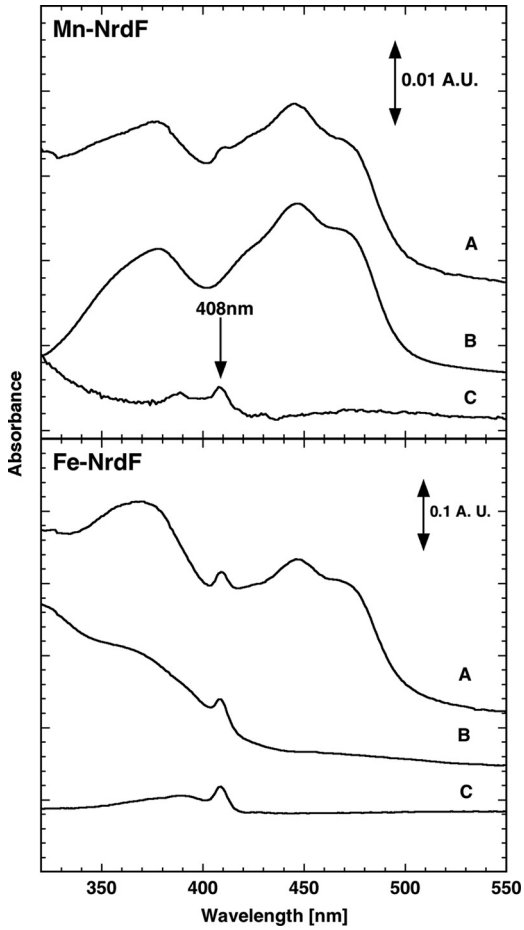

FIGURE 1. **UV-visible absorption of *B. anthracis* Mn-NrdF and Fe-NrdF.** The *upper panel* shows activated Mn-NrdF in the presence of $NrdI_{ox}$ (*trace A*), only $NrdI_{ox}$ (*trace B*), and enzymatically active Mn-NrdF after separation on anion exchange chromatography (*trace C*). The *lower panel* shows Fe-NrdF activated in the presence of $NrdI_{ox}$ (*trace A*) and in the absence of NrdI (*trace B*), and (*trace C*) tyrosyl radical spectrum (after subtraction of spectrum obtained by incubation with radical scavenger hydroxylamine). The spectra in the *upper panel* have been normalized to 2 μM NrdF dimer, and in the *lower panel*, they have been normalized to 10 μM. In the *lower panel*, all spectra correspond to a radical content of 5.9 μM Tyr$^{\bullet}$. *A.U.* denotes absorbance units.

TABLE 1
SPR measured interactions of *B. anthracis* NrdF forms with NrdI

NrdF form	K_D of NrdF-NrdI
	μM
Mn-NrdF	22.6 ± 0.32
Fe-NrdF	29.6 ± 2.12
Apo-NrdF	28.7 ± 2.19

In gel filtration experiments where higher protein and dATP concentrations can be used, we confirmed the monomer/dimer equilibrium for NrdE, the dimer form of NrdF, and the formation of an $\alpha_2\beta_2$ holoenzyme complex in the presence of dATP (Table 2). Densitometric analysis of an SDS-PAGE where the eluted fractions from the 276-kDa $\alpha_2\beta_2$ peak had been separated showed equimolar amounts of NrdE and NrdF proteins (data not shown), and larger complexes were not observed either in gel filtration or in GEMMA. When Mn-NrdF was titrated into a mixture of NrdE + dTTP, $\alpha_2\beta_2$ complex formation was nearly saturated at a molar NrdE-NrdF ratio of 2:1, indicating that some of the *B. anthracis* NrdE was unable to interact with NrdF (supplemental Fig. S8).

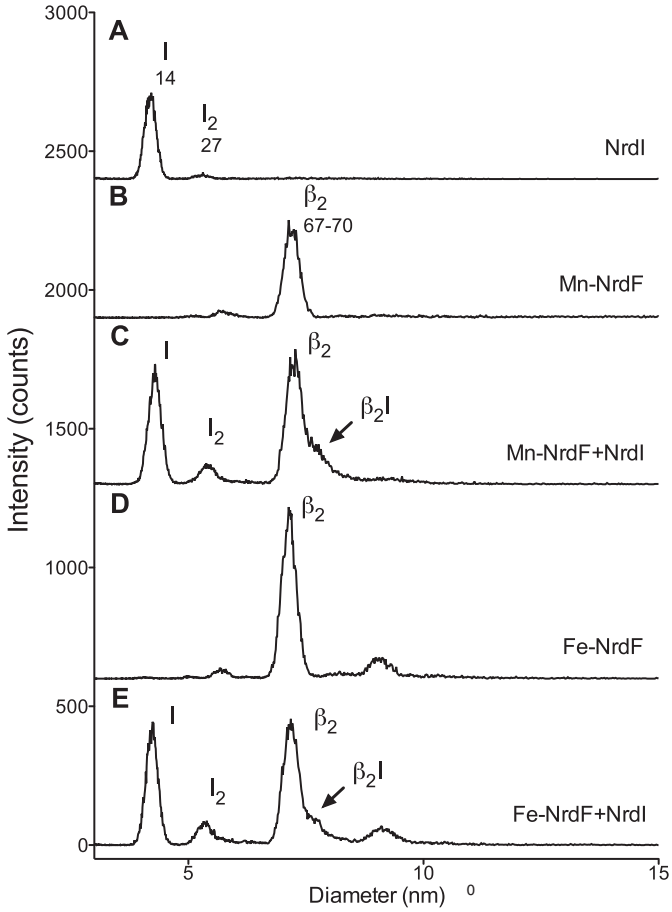

FIGURE 2. **Interactions between *B. anthracis* NrdF and NrdI analyzed by GEMMA.** The NrdI concentration was 0.006 mg/ml in *trace A* and 0.012 mg/ml in *traces C* and *E*. The NrdF concentrations were 0.01 mg/ml in *traces B–E*. The composition and predicted sizes of the species (in kDa) are indicated.

NrdH Mediates High Enzyme Activity of the Mn-NrdF Holoenzyme Complex—Interestingly, the specific activity of the Mn-NrdF form was markedly higher than that of the Fe-NrdF form in the conventional assay with DTT as a chemical reductant (Table 4). The relative enzyme activity per radical was in fact almost five times higher for Mn-NrdF as compared with Fe-NrdF. Even more intriguing is our finding that the physiological reductant NrdH-redoxin promotes an additional 2-fold higher activity for the Mn-NrdF form, but not for the Fe-NrdF form. This effect can be ascribed specifically to the NrdH protein because replacement of DTT as reductant for NrdH with the complete physiological reducing system NrdH, thioredoxin reductase, and NADPH behaved identically to the NrdH + DTT system. The Fe-NrdF protein had the same specific activity with all three reducing systems tested, whereas the Mn-NrdF protein is more active in the presence of NrdH as compared with DTT. Thus, the manganese form has a 10-fold higher activity as compared with the iron form when assayed with NrdH as reductant. Importantly, the presence of equimolar amounts of NrdI did not affect the specific activities (Table 4). To find out whether higher NrdI concentrations affected the specific activity, we titrated NrdI and only found a minor activity decrease at high NrdI excess (supplemental Fig. S9).

The NrdH and thioredoxin reductase were derived from the closely related *B. cereus* species. When assayed in parallel, the *Bacillus* systems had very similar relative activities (Table 4).

TABLE 3

SPR measured interactions of *B. anthracis* NrdF forms with NrdE

NrdF form	K_D NrdE-NrdF
	μM
Mn-NrdF	0.178 ± 0.043
Fe-NrdF	0.195 ± 0.046
Apo-NrdF	0.189 ± 0.026

TABLE 2

***B. anthracis* NrdE, NrdI, Fe-NrdF, and Mn-NrdF interactions and quaternary states as measured by gel filtration and GEMMA**

Protein	Additions[a]	Gel filtration[b] (molecular mass)	GEMMA[c] (molecular mass)	Composition (theoretical molecular mass in kDa in parentheses)
		kDa	kDa	
NrdE	None	82 ± 9	73	α (80)
		196 ± 6		α_2 (160)
NrdE	dATP	ND[d]	81	α (80)
			173	α_2 (160)
Mn-NrdF	None	ND	66–72	β_2 (74)
Fe-NrdF	None	83 ± 6	66	β_2 (74)
NrdI	None	ND	14	I (13)
			27	I_2 (27)
Mn-NrdF + NrdI	None	ND	ND	β_2I (87)
Fe-NrdF + NrdI	None	ND	ND	β_2I (87)
NrdE + Mn-NrdF	dATP	ND	70	α/β_2 (80/74)
			206	$\alpha_2\beta_2$ (234)
NrdE + Fe-NrdF	dATP	80 ± 11	81	α/β_2 (80/74)
		276 ± 12	239	$\alpha_2\beta_2$ (234)

[a] dATP concentration was 0.2 mM in gel filtration and 50 μM in GEMMA.
[b] Protein concentrations were 0.75, 1, 2.5, 5 mg/ml NrdF and 1.5, 2, 2.5, 5 mg/ml NrdE.
[c] Protein concentrations were 0.02 mg/ml (NrdE), 0.01 mg/ml (NrdF), and 0.006–0.012 mg/ml (NrdI).
[d] ND, not determined.

Furthermore the *B. anthracis* and *B. cereus* NrdE and NrdF proteins cross-reacted with preserved activities (data not shown), and the *B. cereus* NrdE batch had a higher activity as compared with the *B. anthracis* NrdE protein regardless of the NrdF protein origin.

To establish whether NrdH interacts strongly with NrdE or the NrdE-Mn-NrdF holoenzyme complex, we again used GEMMA (Fig. 4 and Table 5). NrdH is predominantly a monomer in solution (Fig. 4, *trace A*). No strong or long lived inter-

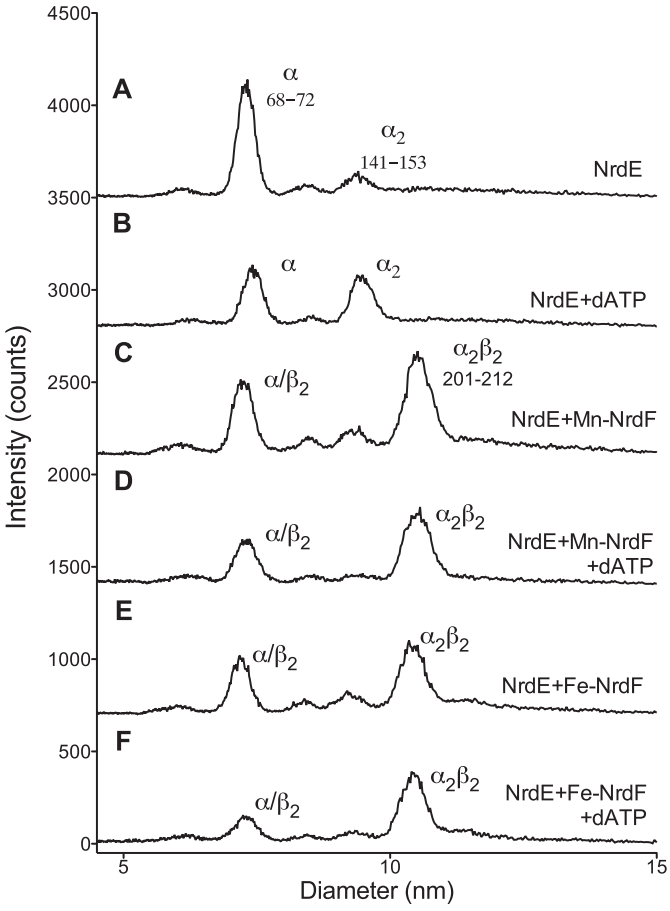

FIGURE 3. **GEMMA of *B. anthracis* Mn-NrdF and Fe-NrdF interactions with NrdE ± dATP.** The NrdE concentration was 0.02 mg/ml, the NrdF concentration was 0.01 mg/ml, and the dATP concentration was 50 μM. The composition and predicted sizes of the species (in kDa) are indicated.

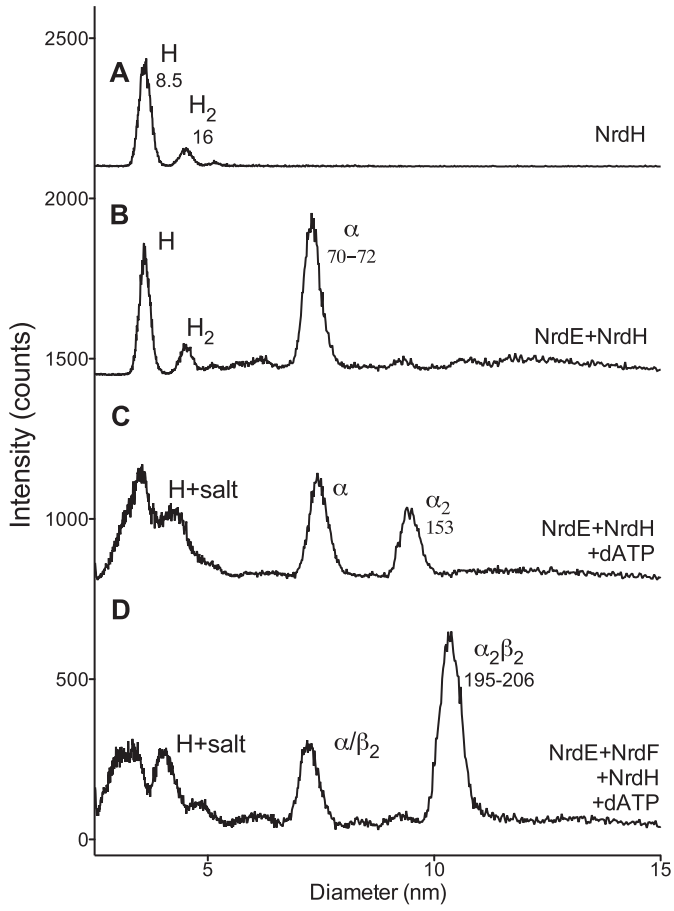

FIGURE 4. **GEMMA of NrdH interaction with NrdE ± dATP and NrdF.** *B. cereus* NrdH concentration was 0.004 mg/ml in *trace A* and 0.008 mg/ml in *traces B–D*. *B. anthracis* NrdE was 0.04 mg/ml, *B. anthracis* Mn-NrdF was 0.02 mg/ml, and dATP was 50 μM. The composition and predicted sizes of the species (in kDa) are indicated.

TABLE 4

Enzyme activity of Mn-NrdF and Fe-NrdF from *B. anthracis* and *B. cereus* in presence or absence of NrdI and with different reducing systems

		B. anthracis		
NrdF/NrdI in assay	Reductant	Specific enzyme activity	Relative enzyme activity per radical (specific activity/Tyr•)[a]	*B. cereus* (relative enzyme activity per radical (specific activity/Tyr•)[b]
		EU/mg		
Mn-NrdF + NrdI	NADPH + NrdH + TR[c]	56 ± 5	1.00[d]	1.00[e]
Mn-NrdF	NADPH + NrdH + TR[c]	70 ± 9	0.95	ND[f]
Fe-NrdF + NrdI	NADPH + NrdH + TR[c]	7.2 ± 0.8	0.07	0.12
Fe-NrdF	NADPH + NrdH + TR[c]	7.2 ± 0.3	0.07	0.13
Mn-NrdF + NrdI	DTT + NrdH[g]	55 ± 11	0.99	0.94
Mn-NrdF	DTT + NrdH[g]	63 ± 4	0.84	ND
Fe-NrdF + NrdI	DTT + NrdH[g]	9.6 ± 0.1	0.09	0.13
Fe-NrdF	DTT + NrdH[g]	8.7 ± 0.1	0.08	0.13
Mn-NrdF + NrdI	DTT	27 ± 0.7	0.49	0.45
Mn-NrdF	DTT	40 ± 7	0.53	ND
Fe-NrdF + NrdI	DTT	8.9 ± 0.2	0.08	ND
Fe-NrdF	DTT	8.4 ± 0.7	0.08	ND

[a] Radical content was 0.30 Tyr•/Mn-NrdF dimer in presence of NrdI, 0.4 Tyr•/Mn-NrdF dimer in absence of NrdI and 0.57 Tyr•/Fe-NrdF dimer.
[b] Radical content was 0.33 Tyr•/Mn-NrdF dimer and 0.7 Tyr•/Fe-NrdF dimer.
[c] Assayed in the presence of *Bacillus cereus* NrdH and thioredoxin reductase (TR).
[d] Specific activity per radical 186 ± 16 EU/mg of Tyr•.
[e] Specific activity 112 ± 7 EU/mg, activity per radical 331 ± 19 EU/mg of Tyr•.
[f] ND, not determined.
[g] Assayed in the presence of *Bacillus cereus* NrdH.

TABLE 5
Interactions and quaternary states of NrdH with NrdE and NrdF as measured by GEMMA

Protein	Additions[a]	GEMMA (molecular mass)[b]	Composition (theoretical molecular mass in kDa in parentheses)
		kDa	
NrdH	None	8.5	H (9)
		16	H_2 (18)
NrdE + NrdH	None	8.5	H (9)
		70–72	α (80)
NrdE + NrdH	dATP	70–74	α (80)
		153	α_2 (160)
NrdE + NrdH + Mn-NrdF	dATP	70–72	α/β_2 (80/74)
		195–206	$\alpha_2\beta_2$ (234)

[a] Protein concentrations were: 0.004 – 0.008 mg/ml (*B. cereus* NrdH), 0.04 mg/ml (*B. anthracis* NrdE), and 0.02 mg/ml (*B. anthracis* NrdF).
[b] When included, dATP was used at a concentration of 50 μM.

action with NrdE could be detected in the absence or presence of the positive allosteric effector dATP (Fig. 4, *traces B* and *C*). Likewise, when NrdH is combined with both NrdE and Mn-NrdF, there is no additional peak present (Fig. 4, *trace D*), indicating that NrdH does not form a strong or long lived interaction with the NrdEF holoenzyme complex.

DISCUSSION

Canonical class I RNRs are encoded in almost all eukaryotic genomes, in quite a number of bacteria, in a few archaea, and in several dsDNA viruses (2, 3). Class I RNRs form tetrameric or higher oligomeric complexes of two subunits: NrdA with the active site and binding sites for allosteric effectors and NrdB with a stable tyrosyl radial adjacent to a diiron-oxo center (1, 10). Two subclasses are known: class Ib, which has been shown recently to harbor the stable tyrosyl radical close to either a dimanganese-oxo center or a diiron-oxo center (15, 16, 31), and class Ic, which harbors the unpaired electron needed to initiate catalysis in a mixed valence Mn^{IV}-Fe^{III} center and which has a phenylalanine residue at the site of the tyrosine residue in the canonical class I RNR (32, 33). This illustrates the diversity of ways that an essential unpaired electron can be safely stored in a metalloprotein matrix. The focus of this study is the class Ib RNR operon in *B. anthracis*, which is encoded by the genes for the catalytic NrdE protein and the radical-containing NrdF protein in an operon that also encodes the flavoprotein NrdI (7, 8, 14). We have earlier shown that the interaction of the NrdE/Fe-NrdF holoenzyme complex is one of the strongest among studied RNRs (30). The essentiality of the NrdI protein was first demonstrated in *Streptococcus pyogenes* (12), and recently, the *E. coli* NrdI was found essential for generation of the Mn_2^{III}/Tyr$^\bullet$ cofactor in *E. coli* NrdF (15, 16, 34). In addition to the Ib operon, *E. coli* also encodes a canonical class I operon and is not dependent upon the class Ib operon during normal growth. Oxidative stress and severe iron limitation may promote the use of class Ib RNR, suggesting that class Ib RNR is essential for growth of *E. coli* under specific conditions (17, 35, 36). The situation is different in *B. anthracis,* the *B. cereus* group, and almost all *Bacillus* spp., which encode a class Ib RNR operon and a class III RNR operon (2). As class III RNRs are strictly anaerobic enzymes, *B. anthracis* and the other *Bacillus* spp. rely solely on their class Ib RNR for dNTP production during aerobic growth (8) In addition, the *B. anthracis* class III operon contains the *nrdD* gene followed by an *nrdG* pseudogene (7), and because the NrdG activase is required for generation of the essential radical in NrdD, the class III enzyme in *B. anthracis* may be non-functional. Recently, Zhang and Stubbe (37) isolated enzymatically active Mn-NrdF from *Bacillus subtilis*, but these studies did not take into account that all *B. subtilis* spp. encode two class Ib operons (2).

Little is known about the metal ion homeostasis in the *B. cereus* group, and it is appropriate to ask whether the *B. anthracis* Ib RNR is cambialistic, *i.e.* can work both as a manganese-dependent enzyme and as an iron-dependent enzyme. We have therefore purified apoNrdF from *B. anthracis*, reconstituted it with either manganese or iron, and compared the properties of Mn-NrdF and Fe-NrdF in regard to interaction with the NrdE component and specific enzyme activity in complex with NrdE. The interaction strength between the NrdE and NrdF subunits was not affected by the metal center, and similar dissociation constants and subunit compositions ($\alpha_2\beta_2$) were recorded in the absence or presence of iron or manganese in the NrdF protein. As the class Ib RNR enzymes lack the dATP inhibition and higher oligomer form-mediating ATP cone domain, it was expected that we did not find higher oligomers than $\alpha_2\beta_2$. However, a striking difference between the *B. anthracis* NrdF forms was that in the presence of the glutaredoxin-like NrdH protein, Mn-NrdF had up to 10-fold higher enzyme activity as compared with Fe-NrdF. We have also validated these results for *B. cereus* Ib RNR.

In many organisms, the glutaredoxin-like NrdH is encoded in the Ib RNR operon together with the genes for NrdI, NrdE, and NrdF, suggesting that NrdH is highly specific for reduction of class Ib RNR. This is the case for *E. coli* as well as *Corynebacterium ammoniagenes* and one of the two Ib operons in *B. subtilis* (38 – 40). However, in *B. anthracis* and the *B. cereus* group, the *nrdH* gene is encoded elsewhere on the chromosome, but a unique specificity for the Ib RNR is plausibly preserved. Our unexpected finding that Mn-NrdF is an order of magnitude more active than Fe-NrdF *in vitro* using conditions that mimic the *in vivo* situation suggests that Mn-NrdF is important *in vivo*. Whether the Fe-NrdF form only exists *in vitro* or whether the NrdF protein in *B. anthracis* is a true cambialistic enzyme remains to be established.

An advantage with the *B. anthracis* Ib RNR as compared with the *E. coli* Ib RNR is that the interaction between NrdF and NrdI is weak (K_D = 23–30 μM), and it was therefore possible to separate NrdF with the Mn_2^{III}/Tyr$^\bullet$ cofactor from $NrdI_{ox}$ after reconstitution. In contrast to what has been reported for the

E. coli class Ib RNR (16), we did not observe any negative effect of NrdI during reconstitution of *B. anthracis* Fe-NrdF or on the enzyme activity of iron- or manganese-activated NrdF. Interestingly, the affinity of NrdI to reconstituted Mn-NrdF was slightly higher as compared with apo- or Fe-NrdF. The recent cloning and expression of the *C. ammoniagenes nrdF* gene in its natural genetic background (31) suggests that the NrdF-to-NrdI interaction here is also weak as Mn-NrdF was isolated without NrdI. The unique characteristics of class Ib enzymes can be exploited in drug development programs targeting RNRs of microbial pathogens, *e.g.* from *B. anthracis* and the *B. cereus* group. *B. anthracis* is an extremely pathogenic bacterium with high proliferation rates during infection. After spore germination, it can easily reach 10^8 cfu/ml in 24 h (41). We have shown in previous work that compounds inhibiting class Ib RNR from *B. anthracis* have bactericidal effects (8, 42). For this reason, it is of particular interest to characterize its RNR components as future targets for antimicrobial therapies.

Acknowledgments—We are grateful to MariAnn Westman for technical assistance and Marta Hammerstad for purifying some of the B. cereus proteins used in this study. B. anthracis Sterne was a kind gift of Åke Forsberg and Ulla Eriksson, Swedish Defence Research Agency Umeå.

REFERENCES

1. Nordlund, P., and Reichard, P. (2006) *Annu. Rev. Biochem.* **75,** 681–706
2. Lundin, D., Torrents, E., Poole, A. M., and Sjöberg, B. M. (2009) *BMC Genomics* **10,** 589
3. Torrents, E., Sahlin, M., and Sjöberg, B. M. (2008) in *Ribonucleotide reductase* (Andersson, K. K. ed) pp. 17–77, Nova Science Publishers, Inc., Hauppauge, NY
4. Uhlin, U., and Eklund, H. (1994) *Nature* **370,** 533–539
5. Logan, D. T., Andersson, J., Sjöberg, B. M., and Nordlund, P. (1999) *Science* **283,** 1499–1504
6. Sintchak, M. D., Arjara, G., Kellogg, B. A., Stubbe, J., and Drennan, C. L. (2002) *Nat. Struct. Biol.* **9,** 293–300
7. Read, T. D., Peterson, S. N., Tourasse, N., Baillie, L. W., Paulsen, I. T., Nelson, K. E., Tettelin, H., Fouts, D. E., Eisen, J. A., Gill, S. R., Holtzapple, E. K., Okstad, O. A., Helgason, E., Rilstone, J., Wu, M., Kolonay, J. F., Beanan, M. J., Dodson, R. J., Brinkac, L. M., Gwinn, M., DeBoy, R. T., Madpu, R., Daugherty, S. C., Durkin, A. S., Haft, D. H., Nelson, W. C., Peterson, J. D., Pop, M., Khouri, H. M., Radune, D., Benton, J. L., Mahamoud, Y., Jiang, L., Hance, I. R., Weidman, J. F., Berry, K. J., Plaut, R. D., Wolf, A. M., Watkins, K. L., Nierman, W. C., Hazen, A., Cline, R., Redmond, C., Thwaite, J. E., White, O., Salzberg, S. L., Thomason, B., Friedlander, A. M., Koehler, T. M., Hanna, P. C., Kolstø, A. B., and Fraser, C. M. (2003) *Nature* **423,** 81–86
8. Torrents, E., Sahlin, M., Biglino, D., Gräslund, A., and Sjöberg, B. M. (2005) *Proc. Natl. Acad. Sci. U.S.A.* **102,** 17946–17951
9. Rofougaran, R., Crona, M., Vodnala, M., Sjöberg, B. M., and Hofer, A. (2008) *J. Biol. Chem.* **283,** 35310–35318
10. Sjöberg, B. M. (2010) *Science* **329,** 1475–1476
11. Cotruvo, J. A., and Stubbe, J. (2011) *Annu. Rev. Biochem.* **80,** 733–767
12. Roca, I., Torrents, E., Sahlin, M., Gibert, I., and Sjöberg, B. M. (2008) *J. Bacteriol.* **190,** 4849–4858
13. Røhr, A. K., Hersleth, H. P., and Andersson, K. K. (2010) *Angew. Chem. Int. Ed. Engl.* **49,** 2324–2327
14. Johansson, R., Torrents, E., Lundin, D., Sprenger, J., Sahlin, M., Sjöberg, B. M., and Logan, D. T. (2010) *FEBS J.* **277,** 4265–4277
15. Boal, A. K., Cotruvo, J. A., Jr., Stubbe, J., and Rosenzweig, A. C. (2010) *Science* **329,** 1526–1530
16. Cotruvo, J. A., Jr., and Stubbe, J. (2010) *Biochemistry* **49,** 1297–1309
17. Martin, J. E., and Imlay, J. A. (2011) *Mol. Microbiol.* **80,** 319–334
18. Sambrook, J., Fritsch, E. F., and Maniatis, T. (1989) *Molecular Cloning: A Laboratory Manual*, 2nd Ed., Cold Spring Harbor Laboratory Press
19. Nord, D., Torrents, E., and Sjöberg, B. M. (2007) *J. Bacteriol.* **189,** 5293–5301
20. Røhr, Å. K. (2010) *Structural and Spectroscopic Studies of the Flavoprotein NrdI, Thioredoxin BC3987, and Ribonucleotide Reductase Diiron-Protein R2.* Ph.D thesis, University of Oslo, Oslo, Norway
21. Tomter, A. B., Bell, C. B., 3rd, Røhr, A. K., Andersson, K. K., and Solomon, E. I. (2008) *Biochemistry* **47,** 11300–11309
22. Tomter, A. B. (2010) *Spectroscopic Studies of the Ribonucleotide Reductase R2-Subunits from Mammals, Virus, and Bacteria*. Ph.D thesis, University of Oslo, Oslo, Norway
23. Magnusson, K. E., and Edebo, L. (1976) *Biotechnol. Bioeng.* **18,** 865–883
24. Jordan, A., Pontis, E., Atta, M., Krook, M., Gibert, I., Barbé, J., and Reichard, P. (1994) *Proc. Natl. Acad. Sci. U.S.A.* **91,** 12892–12896
25. Jordan, A., Pontis, E., Aslund, F., Hellman, U., Gibert, I., and Reichard, P. (1996) *J. Biol. Chem.* **271,** 8779–8785
26. Yang, F., Curran, S. C., Li, L. S., Avarbock, D., Graf, J. D., Chua, M. M., Lu, G., Salem, J., and Rubin, H. (1997) *J. Bacteriol.* **179,** 6408–6415
27. Fieschi, F., Torrents, E., Toulokhonova, L., Jordan, A., Hellman, U., Barbe, J., Gibert, I., Karlsson, M., and Sjöberg, B. M. (1998) *J. Biol. Chem.* **273,** 4329–4337
28. Thelander, L., Sjöberg, B. M., and Eriksson, S. (1978) *Methods Enzymol.* **51,** 227–237
29. Rofougaran, R., Vodnala, M., and Hofer, A. (2006) *J. Biol. Chem.* **281,** 27705–27711
30. Crona, M., Furrer, E., Torrents, E., Edgell, D. R., and Sjöberg, B. M. (2010) *Protein Eng. Des. Sel.* **23,** 633–641
31. Cox, N., Ogata, H., Stolle, P., Reijerse, E., Auling, G., and Lubitz, W. (2010) *J. Am. Chem. Soc.* **132,** 11197–11213
32. Jiang, W., Yun, D., Saleh, L., Barr, E. W., Xing, G., Hoffart, L. M., Maslak, M. A., Krebs, C., and Bollinger, J. M., Jr. (2007) *Science* **316,** 1188–1191
33. Voevodskaya, N., Galander, M., Högbom, M., Stenmark, P., McClarty, G., Gräslund, A., and Lendzian, F. (2007) *Biochim. Biophys. Acta* **1774,** 1254–1263
34. Cotruvo, J. A., and Stubbe, J. (2011) *Biochemistry* **50,** 1672–1681
35. Grass, G., Franke, S., Taudte, N., Nies, D. H., Kucharski, L. M., Maguire, M. E., and Rensing, C. (2005) *J. Bacteriol.* **187,** 1604–1611
36. Anjem, A., Varghese, S., and Imlay, J. A. (2009) *Mol. Microbiol.* **72,** 844–858
37. Zhang, Y., and Stubbe, J. (2011) *Biochemistry* **50,** 5615–5623
38. Jordan, A., Aslund, F., Pontis, E., Reichard, P., and Holmgren, A. (1997) *J. Biol. Chem.* **272,** 18044–18050
39. Torrents, E., Roca, I., and Gibert, I. (2003) *Microbiology* **149,** 1011–1020
40. Härtig, E., Hartmann, A., Schätzle, M., Albertini, A. M., and Jahn, D. (2006) *Appl. Environ. Microbiol.* **72,** 5260–5265
41. Mock, M., and Fouet, A. (2001) *Annu. Rev. Microbiol.* **55,** 647–671
42. Torrents, E., and Sjöberg, B. M. (2010) *Biol. Chem.* **391,** 229–234

Supplementary material

NrdH-REDOXIN MEDIATES HIGH ENZYME ACTIVITY IN MANGANESE-RECONSTITUTED RIBONUCLEOTIDE REDUCTASE FROM *Bacillus anthracis*

Mikael Crona[1], Eduard Torrents[1,2§], Åsmund K Røhr[3§], Anders Hofer[4], Ernst Furrer[1#], Ane B Tomter[3], K Kristoffer Andersson[3], Margareta Sahlin[1] and Britt-Marie Sjöberg[1]*

From [1]Department of Molecular Biology and Functional Genomics, Arrhenius Laboratories for Natural Sciences, Stockholm University, SE-10691 Stockholm, Sweden, [2]Cellular Biotechnology, Institute for Bioengineering of Catalonia, Baldiri Reixac 15-21, ES-08080 Barcelona, Spain, [3]Department of Molecular Biosciences, University of Oslo, NO-0316 Oslo, Norway, [4]Department of Medical Biochemistry & Biophysics, Umeå University, SE-90187 Umeå, Sweden.

Table of contents:

Figure S1. The *B. anthracis nrdIEF* operon. IVS denotes intervening sequence, and HEG denotes homing endonuclease gene. Primers described in Material & Methods and used for construction of the NrdE expression plasmid pETS146 are shown.

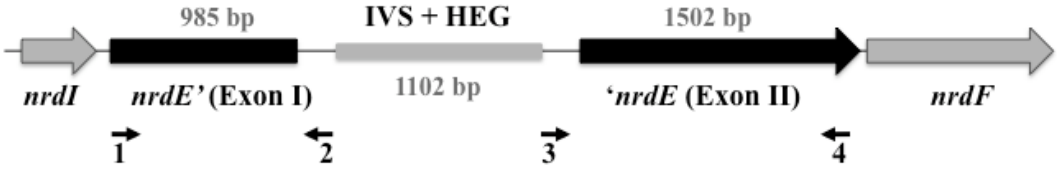

Figure S2. SDS-PAGE of purified *B. anthracis* NrdE. Lane 1, protein ladder (Fermentas); lane 2, crude extract (5 µg) of *E. coli* culture overproducing *B. anthracis* NrdE; lane 3, purified *B. anthracis* NrdE (3 µg).

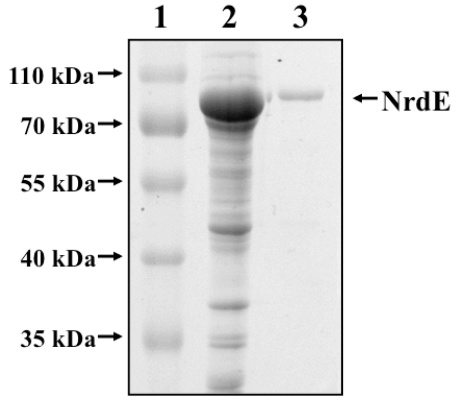

Figure S3. Separation of *B. anthracis* NrdI from Mn-reconstituted NrdF using MonoQ anion exchange chromatography. Separation of the NrdI protein and the NrdF protein with radical and lacking radical is indicated. The absorption is shown in mAU and the gradient from 0-60% 1 M KCl is shown.

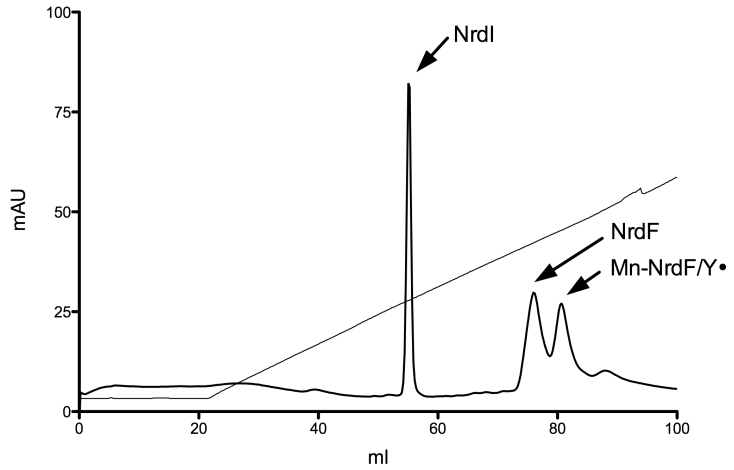

Figure S4. Dithiothreitol and pH dependence of the *B. anthracis* RNR enzyme assay. A) Dependence on dithiothreitol, B) dependence on pH. All incubations were done under standard conditions described in the material and methods using 7.4 µM of NrdE and 16.2 µM of Fe-NrdF.

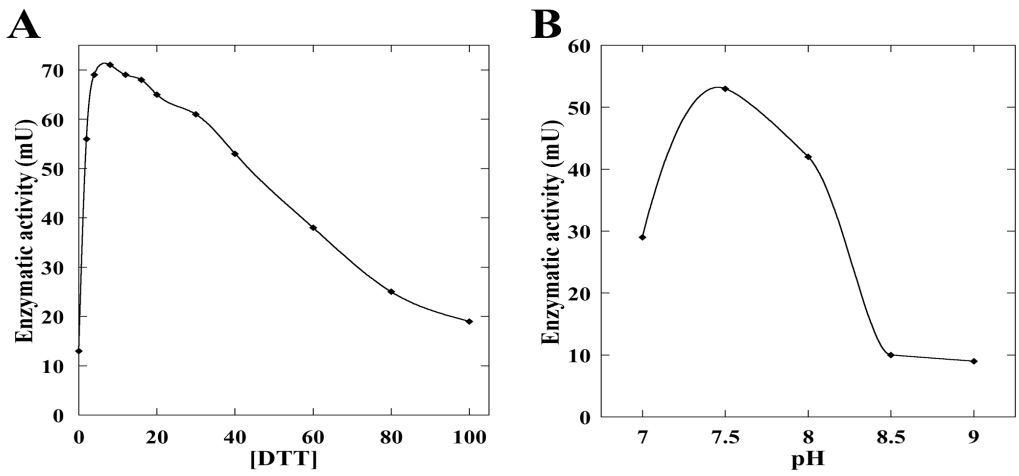

Figure S5. *B. anthracis* NrdI/NrdF interaction SPR sensorgrams and steady state plots. 2.5 μM-60 μM of NrdI was injected over immobilized biotinylated NrdF proteins.

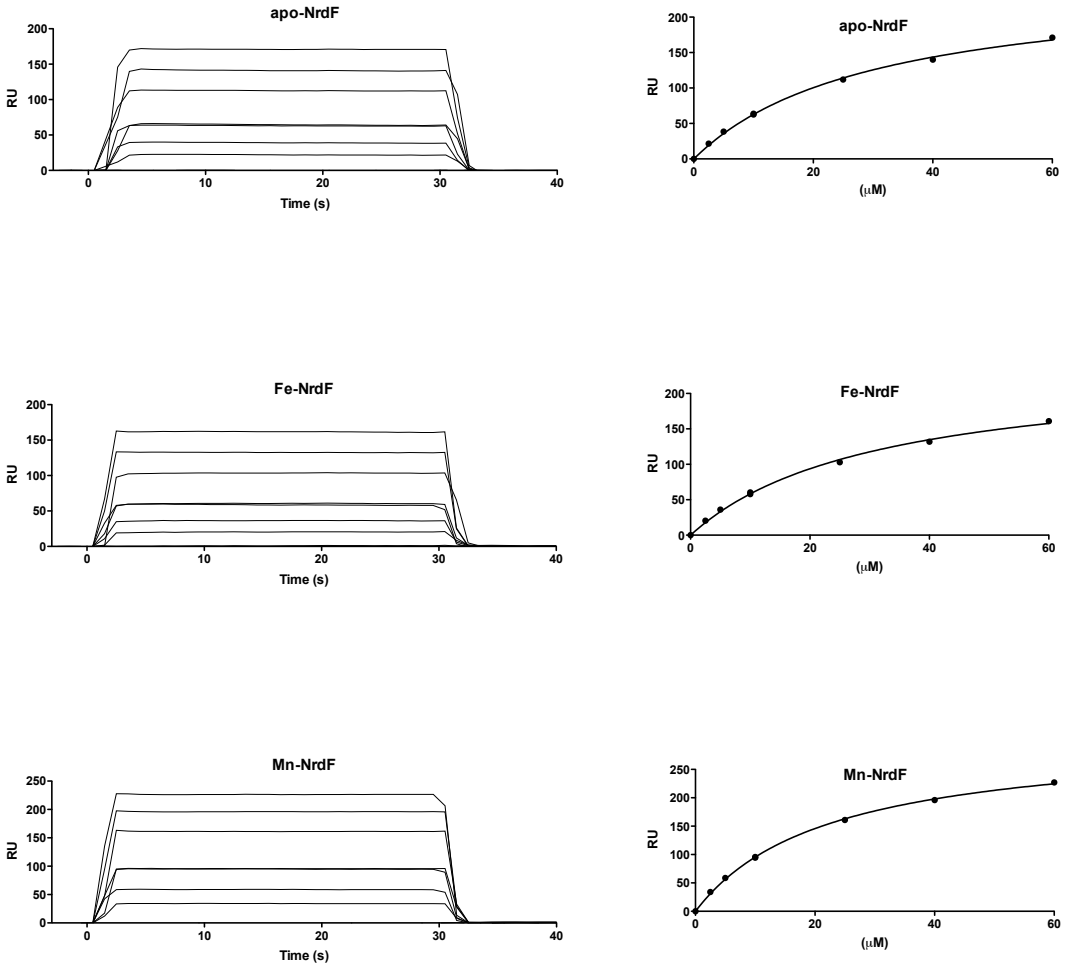

Figure S6. *B. anthracis* NrdE/NrdF interaction SPR sensorgrams and steady state plots. 0.025 μM-2 μM of NrdE was injected over immobilized biotinylated NrdF proteins.

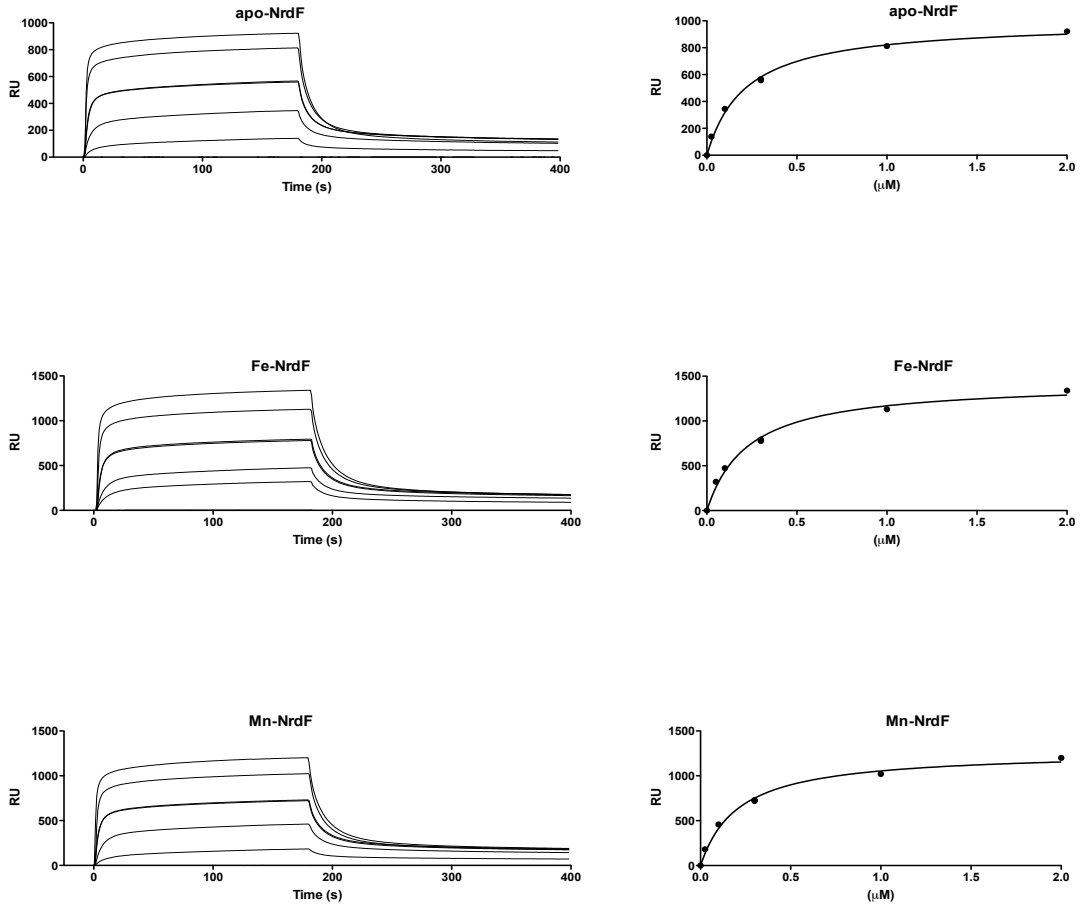

Figure S7. Dimerization of *B. anthracis* NrdE is promoted by effectors but not by substrate. GEMMA analyses of 0.02 mg/ml NrdE alone and in the presence 25 μM dGTP, 50 μM dTTP, or 50 μM CDP. The composition and predicted sizes of the species (in kDa) are indicated.

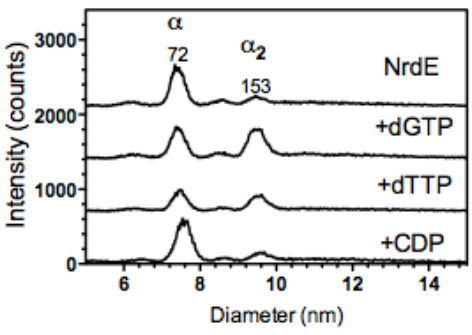

Figure S8. Titration of *B. anthracis* NrdE+dTTP with increasing concentrations of Mn-NrdF. GEMMA analyses of 0.02 mg/ml NrdE, 50 µM dTTP, in the presence of varying concentrations of Mn-NrdF (0.0053 and 0.017 mg/ml). The composition and predicted sizes of the species (in kDa) are indicated.

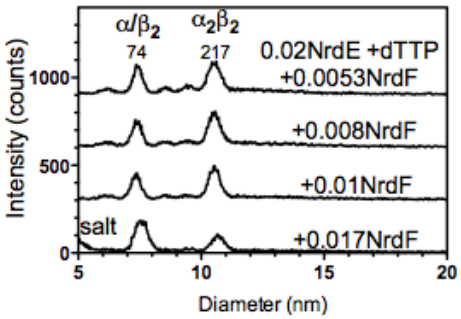

Figure S9. Activity of *B. anthracis* NrdF in presence of increasing NrdI concentrations. The activity of Fe and Mn reconstituted *B. anthracis* NrdF proteins were only marginally effected by an NrdI excess of up to 8 times. Specific activity in absence of NrdI: Mn-NrdF 67.83 U/mg and Fe-NrdF 10.67 U/mg.